ELSEVIER

International Journal of Heat and Fluid Flow 21 (2000) 620–626

International Journal of HEAT AND FLUID FLOW

www.elsevier.com/locate/ijhff

Numerical simulation of transonic buffet flows using various turbulence closures

G. Barakos, D. Drikakis *,[1]

Department of Engineering, Queen Mary and Westfield College, University of London, London E1 4NS, UK

Abstract

The paper presents a numerical investigation of buffet flows using various turbulence models, including linear and non-linear low-*Re* eddy-viscosity models (EVM). The accuracy of the models is assessed against experimental data for transonic flows around the NACA-0012 aerofoil. The study shows that non-linear two-equation models in conjunction with functional c_μ coefficient for the calculation of the eddy-viscosity (henceforth labelled NL-c_μ), provide satisfactory results for transonic buffet flows. The computations also reveal that the Spalart–Allmaras one-equation model provides comparable results to the NL-c_μ models, while larger inaccuracies are introduced by linear and non-linear models based on constant c_μ coefficient. Moreover, the buffet onset boundaries are similarly predicted by the one-equation and NL-c_μ models. The study has been performed using a second-order time accurate implicit-unfactored method which solves in a coupled fashion the Navier–Stokes and turbulence transport equations. The spatial discretisation of the equations is obtained by a Riemann solver in combination with a third-order upwind scheme.

Keywords: Buffet; Transonic flows; Turbulence; Eddy-viscosity turbulence models

1. Introduction

Significant efforts to validate turbulence models in steady aerodynamic flows have been spent over the past decade (e.g., Haase et al., 1993; Bardina et al., 1997; Leschziner, 1998; Barakos and Drikakis, 1998a, 2000b, amongst others). However, much less information has been accumulated in connection with the validation of turbulence models in unsteady aerodynamic flows featuring buffet and/or dynamic-stall. Concerning dynamic-stall, recent studies (Barakos and Drikakis, 1999, 2000a) using a variety of low-Re linear and non-linear eddy-viscosity models (EVM), have been performed. These studies revealed that non-linear EVMs can indeed offer better accuracy than algebraic and one-equation models, in predicting dynamic-stall both in subsonic and transonic flows over pitching and oscillating aerofoils. On the other hand, buffet computations have so far been performed by using, mainly, algebraic turbulence models (Edwards, 1996; Girodroux-Lavigne and LeBalleur, 1988). Therefore, the present study has been initiated in order to assess more advanced turbulence closures in transonic buffet flows around aerofoils.

Transonic buffet appears in many aeronautical applications such as internal flows in compressor passages, around turbomachinery blades as well as in external flows over aircraft wings. The aerodynamic performance in these applications depends strongly on the unsteady shock/boundary-layer interaction. The latter may change position around the aerofoil due to the self-excited shock oscillations. Accurate predictions of such flow phenomena is of significant technological importance and their simulation remains a challenging problem due to the complex physics involved. The accuracy of the numerical predictions is dictated both by the accuracy/properties of the numerical discretisation scheme as well as by the accuracy of the turbulence model. The present work focuses on investigating accuracy issues associated with the turbulence model.

Experience from steady flows using algebraic turbulence models has shown that such modelling of turbulence does not provide satisfactory results in most cases. Linear low-*Re* two-equation models (Launder and Sharma, 1974; Nagano and Kim, 1988) seem to offer the best balance between accuracy and computational cost, but are not able to capture effects arising from normal-stress anisotropy and are less able to predict separation in adverse pressure gradient and shock/boundary-layer interaction (Liou and Shih, 1996; Marvin and Huang, 1996).

At present non-linear models seem to be one of the principal routes for advanced modelling of turbulence beyond the linear EVM. Such models take into account streamline curvature and swirl, as well as history effects. So far, non-linear

* Corresponding author. Tel.: +44-20-7882-5194; fax: +44-20-8983-1007.

E-mail address: d.drikakis@qmw.ac.uk (D. Drikakis).

[1] Part of this work was carried out when the authors were at Department of Mechanical Engineering, UMIST, Manchester M60 1QD, UK.

0142-727X/00/$ - see front matter
PII: S0142-727X(00)00053-9

Notation

α_{ij}	Reynolds stress anisotropy tensor, $\alpha_{ij} \equiv \overline{u_i'u_j'}/k - (2/3)\delta_{ij}$
c	chord length of the aerofoil
c_l	lift coefficient
c_m	quarter-chord moment coefficient
e	total energy of the fluid per unit volume
E, G, E_v, G_v	inviscid and viscous fluxes, in curvilinear coordinates
$\tilde{E}$, $\tilde{G}$, $\tilde{E}_v$, $\tilde{G}_v$	inviscid and viscous fluxes, in Cartesian coordinates
H	source term due to turbulence modelling
J	Jacobian of transformation from Cartesian to curvilinear coordinates
k	turbulent kinetic energy, $k = \overline{u_i'u_i'}/2$
M	freestream Mach number
p	pressure
Pr	Prandtl number, $Pr = \rho\mu c_p/k$
Pr_t	turbulent Prandtl number, $Pr_t = \rho\mu_t c_p/k$
t	time
Re	Reynolds number, $Re = \rho U c/\mu$
$\tilde{R}_t$	near-wall Reynolds number, $\tilde{R}_t = \rho k^2/\mu\tilde{\epsilon}$
S	strain invariant, $S \equiv \sqrt{S_{ij}S_{ij}/2}$
S_{ij}	strain tensor, $S_{ij} \equiv \partial u_i/\partial x_j + \partial u_j/\partial x_i$
U	velocity
u_i	mean velocity component in the x_i-direction, $(i = 1, 2)$
$-\rho\overline{u_i'u_j'}$	Reynolds-stress tensor
x_i	cartesian coordinates $(i = 1, 2, x = x_1, z = x_2)$

Greeks

α	angle of attack
ϵ	dissipation rate of k
$\tilde{\epsilon}$	isotropic dissipation rate of k, $\tilde{\epsilon} \equiv \epsilon - \hat{\epsilon}$, $\hat{\epsilon} \equiv 2(\mu/\rho)(\partial\sqrt{k}/\partial x_j)^2$
μ	coefficient of dynamic viscosity
μ_T	eddy-viscosity
ρ	density
τ	time in the curvilinear coordinate system
τ_{ij}	total stress tensor
τ_{lij}	molecular stress tensor
τ_{tij}	turbulent Reynolds stress tensor
ξ_i, ζ	curvilinear coordinates
Ω	vorticity invariant, $\Omega \equiv \sqrt{\Omega_{ij}\Omega_{ij}/2}$
Ω_{ij}	vorticity tensor, $\Omega_{ij} \equiv \partial u_i/\partial x_j - \partial u_j/\partial x_i$
ω	specific turbulent dissipation rate, turbulent frequency, $\omega \equiv \epsilon/k$

models have been validated for steady flows, mainly two-dimensional and incompressible, (e.g., Craft et al., 1996, amongst others), while more recently experience has been acquired from applications to compressible flows with shock/boundary-layer interaction (e.g., Barakos and Drikakis, 2000b).

In the present work, various turbulence closures including algebraic, one-equation as well as linear and non-linear low-Re two-equation models, are validated in transonic buffet flows. The assessment of the models is performed against experimental results for buffet around the NACA-0012 aerofoil at Reynolds number $Re = 10^7$, a range of Mach numbers between 0.7 and 0.85, and for incidence angles between 0° and 5° (McDevitt and Okuno, 1985).

2. Numerical method

The numerical simulations have been carried out using an implicit CFD solver (Barakos and Drikakis, 1998b, 1999) developed for unsteady and turbulent aerodynamic flows. The main feature of the method is the strong coupling of turbulence models with the Navier–Stokes equations, via an implicit unfactored scheme and a Riemann solver, the latter being used in conjunction with a third-order upwind interpolation scheme (Drikakis and Durst, 1994).

The compressible Navier–Stokes equations for a two-dimensional curvilinear co-ordinate system (ξ, η), in conjunction with the transport equations of the turbulence model, are written in matrix form as

$$\frac{\partial U}{\partial t} + \frac{\partial E}{\partial \xi} + \frac{\partial G}{\partial \zeta} = \frac{\partial R}{\partial \xi} + \frac{\partial S}{\partial \zeta} + H. \tag{1}$$

U is the six-component vector of the conservative variables

$$U = J(\rho, \rho u, \rho w, e, \rho k, \rho\tilde{\epsilon})^{\mathrm{T}}, \tag{2}$$

where ρ is the density, u, w are the velocity components in the x- and z-directions, respectively, e the total energy per unit volume, k the turbulent kinetic energy and $\tilde{\epsilon}$ is the isotropic part of the turbulent dissipation rate (in the case of the Launder–Sharma model).

The matrix $H = J\tilde{H}$ has non-zero entries for the source terms of the turbulence model equations. J is the Jacobian of the transformation from Cartesian to curvilinear co-ordinate system. E, G and R, S are the inviscid and viscous fluxes, respectively. The total energy per unit volume e is given by $e = \rho i + (1/2)\rho(u^2 + w^2) + \rho k$, where i is the specific internal energy. The pressure is calculated by the ideal gas equation of state.

A third-order upwind scheme in conjunction with a characteristic-based flux averaging is used to calculate the inviscid fluxes at the cell faces (Eberle et al., 1992; Drikakis and Durst, 1994). Limiters based on the squares of pressure derivatives have been used in detecting shocks and contact discontinuities. An implicit-unfactored solver (Barakos and Drikakis, 1998b, 1999) has been employed for the solution of the equations. A sequence of approximations q^ν such that: $\lim_{\nu>1} q^\nu \to U^{n+1}$ is defined between two time steps n and $n+1$. Using implicit time discretization and after linearizing the fluxes around the sub-iteration state ν the following form is derived:

$$\frac{\Delta q}{\Delta t} + (A^\nu_{\mathrm{inv}}\Delta q)_\xi + (C^\nu_{\mathrm{inv}}\Delta q)_\zeta - (A^\nu_{\mathrm{vis}}\Delta q)_\xi - (C^\nu_{\mathrm{vis}}\Delta q)_\zeta = \mathrm{RHS}, \tag{3}$$

where

$$\mathrm{RHS} = -\left(\frac{q^\nu - U^n}{\Delta t} + E^\nu_\xi + G^\nu_\zeta - R^\nu_\xi - S^\nu_\zeta - H^\nu\right), \tag{4}$$

$$\Delta q = q^{\nu+1} - q^\nu \tag{5}$$

and

$$A_{\mathrm{inv}} = \frac{\partial E}{\partial U}, \quad C_{\mathrm{inv}} = \frac{\partial G}{\partial U}, \quad A_{\mathrm{vis}} = \frac{\partial R}{\partial U}, \quad C_{\mathrm{vis}} = \frac{\partial S}{\partial U}. \tag{6}$$

At each time step the final system of algebraic equations is solved by a point Gauss–Seidel relaxation scheme. According to the present method, the transport equations for the turbulence model are solved coupled with the fluid flow equations.

This strategy provides fast convergence and compact numerical implementation.

For unsteady flow simulations the discretisation of the time derivative is obtained by a second-order scheme (Barakos and Drikakis, 1999)

$$\frac{1.5U^{n+1}-2U^{n}+0.5U^{n-1}}{\Delta\tau} = -\left(E_{\xi}^{n+1}+F_{\eta}^{n+1}-R_{\xi}^{n+1}-S_{\eta}^{n+1}-H^{n+1}\right). \quad (7)$$

In time accurate computations, the time marching must be performed using the same time step in all cells of the computational domain. This global time step is defined for a given CFL number by

$$\Delta\tau \leqslant \Delta\tau_{\max} = \min\left(J\frac{CFL}{\lambda_{\max}+2(\mu c_{\mathrm{p}}/Pr)\sqrt{(\xi_x^2+\xi_z^2+\zeta_x^2+\zeta_z^2)}}\right)_{i,k}, \quad (8)$$

where $\lambda_{\max}$ is the maximum eigenvalue calculated using the solution from the previous time step.

3. Turbulence modelling

In the present study, the following models have been employed: the algebraic Baldwin and Lomax (1978) model, the one-equation model of Spalart and Allmaras (1992), the Launder and Sharma (1974) and Nagano and Kim (1988) linear k–ϵ models, as well as the k–ω version (Sofialidis and Prinos, 1997) of the non-linear eddy-viscosity model of Craft et al. (1996).

In the case of linear EVM the stress tensor τ_{ij} is modelled using the Boussinesq approximation

$$\tau_{ij}=\tau_{ij}^{\mathrm{l}}+\tau_{ij}^{\mathrm{R}}, \quad (9)$$

where

$$\tau_{ij}^{\mathrm{l}}=\mu\left(\frac{\partial u_i}{\partial x_j}+\frac{\partial u_j}{\partial x_i}\right)-\frac{2}{3}\mu\frac{\partial u_k}{\partial x_k}\delta_{ij}, \quad (10)$$

$$\tau_{ij}^{\mathrm{R}}=\mu_{\mathrm{T}}\left(\frac{\partial u_i}{\partial x_j}+\frac{\partial u_j}{\partial x_i}\right)-\frac{2}{3}\mu_{\mathrm{T}}\frac{\partial u_k}{\partial x_k}\delta_{ij}-\frac{2}{3}\rho_k\delta_{ij} \quad (11)$$

and μ_{T} is the eddy-viscosity.

Non-linear EVM use an expansion of the Reynolds stress components in terms of the mean strain-rate and rotation tensors

$$S_{ij}=\left(U_{i,j}+U_{j,i}\right)/2, \quad \Omega_{ij}=\left(U_{i,j}-U_{j,i}\right)/2. \quad (12)$$

In the case of the non-linear k–ϵ EVM of Craft et al. (1996) a cubic expansion for the anisotropy of the Reynolds stress tensor, $a_{ij}\equiv\overline{u_iu_j}/k-(2/3)\delta_{ij}$, is employed

$$\begin{aligned} a_{ij} = & -\frac{\mu_{\mathrm{T}}}{\rho k}S_{ij}+c_1\frac{\mu_{\mathrm{T}}}{\rho\tilde{\epsilon}}\left\{S_{ik}S_{kj}-\frac{1}{3}S_{kl}S_{kl}\delta_{ij}\right\} \\ & +c_2\frac{\mu_{\mathrm{T}}}{\rho\tilde{\epsilon}}\left(\Omega_{ik}S_{kj}+\Omega_{jk}S_{ki}\right)+c_3\frac{\mu_{\mathrm{T}}}{\rho\tilde{\epsilon}}\left(\Omega_{ik}\Omega_{jk}-\frac{1}{3}\Omega_{lk}\Omega_{lk}\delta_{ij}\right) \\ & +c_4\frac{\mu_{\mathrm{T}}k}{\rho\tilde{\epsilon}^2}\left(S_{ki}\Omega_{lj}+S_{kj}\Omega_{li}\right)S_{kl} \\ & +c_5\frac{\mu_{\mathrm{T}}k}{\rho\tilde{\epsilon}^2}\left(\Omega_{il}\Omega_{lm}S_{mj}+S_{il}\Omega_{lm}\Omega_{mj}-\frac{2}{3}S_{lm}\Omega_{mn}\Omega_{nl}\delta_{ij}\right) \\ & +c_6\frac{\mu_{\mathrm{T}}k}{\rho\tilde{\epsilon}^2}S_{ij}S_{kl}S_{kl}+c_7\frac{\mu_{\mathrm{T}}k}{\rho\tilde{\epsilon}^2}S_{ij}\Omega_{kl}\Omega_{kl}. \end{aligned} \quad (13)$$

This cubic expansion has been utilized here to calculate the components of the Reynolds-stress tensor $-\overline{\rho}\,\overline{u_iu_j}$. In the above, S_{ij} and Ω_{ij} are the strain and vorticity tensors, while $\tilde{S}$ and $\tilde{\Omega}$ are their normalized invariants

$$\tilde{S}\equiv\frac{k}{\tilde{\epsilon}}\sqrt{S_{ij}S_{ij}/2}, \quad \tilde{\Omega}\equiv\frac{k}{\tilde{\epsilon}}\sqrt{\Omega_{ij}\Omega_{ij}/2}, \quad (14)$$

and the coefficients c_i take the values: $c_1=-0.1, c_2=0.1$, $c_3=0.26, c_4=-10c_{\mu}^2$. The eddy viscosity is calculated by $\mu_{\mathrm{T}}=c_{\mu}\rho f_{\mu}(k^2/\tilde{\epsilon})$, where

$$c_{\mu}=\frac{0.3[1-\exp\{-0.36\exp(0.75\eta)\}]}{1+0.35\eta^{1.5}}, \quad (15)$$

$$f_{\mu}=1-\exp\left\{-\left(\frac{\tilde{R}_{\mathrm{t}}}{90}\right)^{1/2}-\left(\frac{\tilde{R}_{\mathrm{t}}}{400}\right)^{2}\right\}, \quad (16)$$

$$\eta=\max\left(\tilde{S},\tilde{\Omega}\right). \quad (17)$$

Such functional form of c_{μ} was found to be beneficial in flows far from equilibrium and similar conclusions have also been reported by Liou and Shih (1996), Huang (1999) and Bardina et al. (1997) for a variety of compressible flows. The non-linear eddy-viscosity model of Sofialidis and Prinos (1997) is actually the k–ω version of the non-linear k–ϵ model of Craft et al. (1996).

4. Simulation of transonic buffet

4.1. Test cases

Computations were carried out for the experimental cases of McDevitt and Okuno (1985). Their experiments have been performed for the NACA-0012 aerofoil at Mach numbers between 0.7 and 0.8, angles of incidence less than 5° and Re_{c} number between 1 and 14 millions. McDevitt and Okuno identified the incidence-angle and Mach number as the most important parameters for the buffet onset. Their wind-tunnel results are particularly suitable for validating CFD codes because they are free of wall effects in contrast to previous experimental studies (McDevitt et al., 1976).

McDevitt and Okuno (1985) organized their experiments in six sets and the corresponding parameters are shown in Table 1. For the sets numbered as 4, 5 and 6, buffet was reported and, consequently, these sets were considered in the present work. As has also been reported by Mateer et al. (1992), the effects of boundary-layer tripping on the obtained results for Re about 10^6, is negligible. Therefore, in the present study computations were carried out for Reynolds number $Re=10^6$ which provides fully turbulent flow (McDevitt and Okuno, 1985).

Table 1
Nominal conditions for the experiments of McDevitt and Okuno (1985)

Set	Incidence α (deg)	Mach number	Re ($\times10^{-6}$)
1	2	0.75	1.2–13.9
2	0	0.75	4.0–12.2
3	0	0.8	1.2.0–12.1
4	1	0.8	1.0–10.3
5	2	0.775	1.0–9.9
6	4	0.725	1.0–9.3

4.2. Results

Flow unsteadiness around a lifting surface may originate from the motion of the boundary or from unsteady free-stream conditions. However, in the case of buffet the induced unsteadiness is due to flow non-linearities associated with certain combinations of *Re*, Mach number, and angle of incidence. In the case of transonic buffet, the self-excited shock oscillations are also associated with shock/boundary-layer interaction and flow separation. It is thus important for a turbulence model to

Table 2
Details of the computational grids employed in the calculations; grid G4 was selected for buffet calculations

Grid	*i*-direction	*k*-direction	Far-field location
G1	180	60	5c
G2	241	80	5c
G3	291	85	7c
G4	361	90	7c

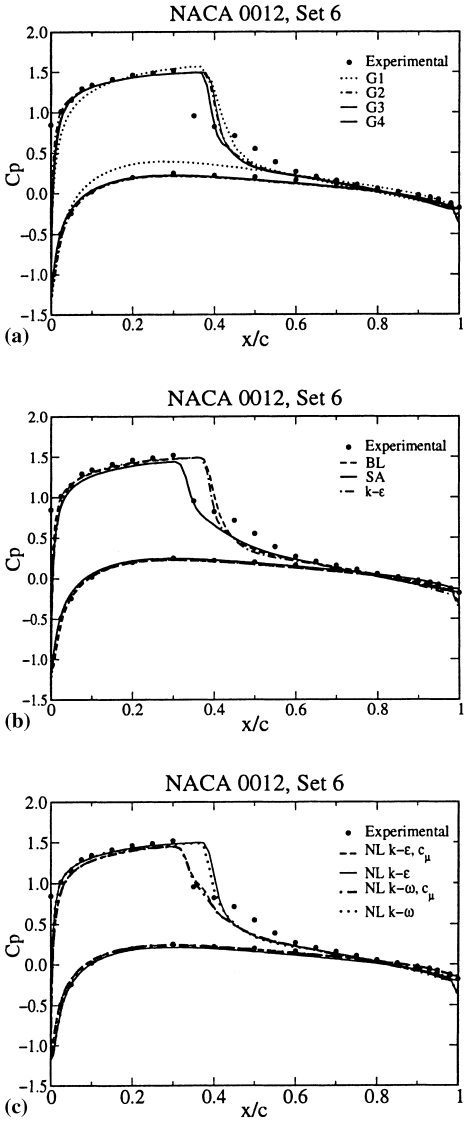

Fig. 1. Pressure coefficient distribution around the NACA-0012 aerofoil: (a) grid size effects, (b) comparisons between linear turbulence models (c) comparisons between non-linear turbulence models; The experimental data are from McDevitt and Okuno (1985) ($Re = 10^7$, $M = 0.775$, $\alpha = 4°$).

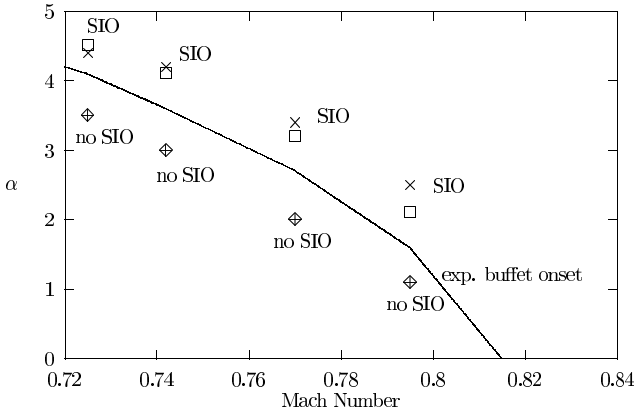

Fig. 2. Buffet onset for the NACA-0012 aerofoil ($Re_c = 10^7$, $M = 0.775$, $\alpha = 4°$). Solution obtained using the SA model (crosses) and the non-linear k–ω model (squares). The experimental data are from McDevitt and Okuno (1985). SIO stands for shock-induced oscillation.

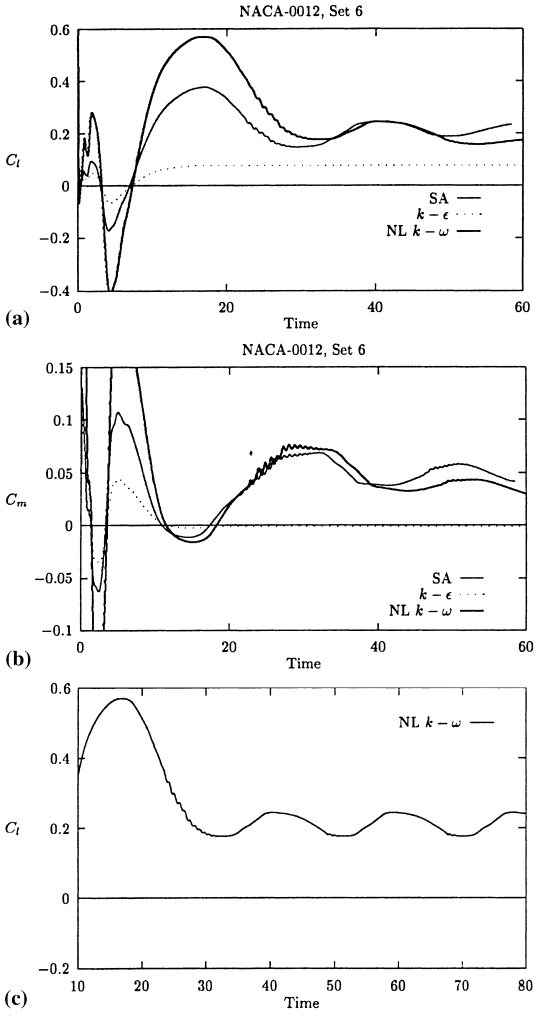

Fig. 3. Oscillating airloads for the NACA-0012 aerofoil: (a) lift coefficient, (b) moment coefficient, (c) lift coefficient for a long time interval using the NL k–ω model ($Re = 10^7$, $M = 0.775$, $\alpha = 4°$).

predict accurately the separation induced by the interaction of the shock with the boundary layer and, subsequently, the buffet onset.

In the present study, several computational grids have been employed to ensure grid-independent solutions and their details are given in Table 2. In addition, calculations have been performed for various dimensions of the computational domain to ensure independence of the solution from the far-field boundary conditions. For buffet predictions the grid G4 (Table 2) was used.

In Fig. 1, the C_p distributions, for $M = 0.775$ and $\alpha = 4°$, using various closures and different grids are compared with the experimental results. For this Mach number and incidence angle, the flow has been found (McDevitt and Okuno, 1985) to be steady and all turbulence models predicted steady flow, as well. As can be seen, none of the models was able to capture exactly the experimental shock position. The non-linear models were used in conjunction with both functional c_μ (Eq. (15)) and constant c_μ ($c_\mu = 0.09$) coefficient. When the models were employed with a constant c_μ, were found to give results (Fig. 1(c)) similar to the ones obtained by the linear k–ϵ and algebraic models (Fig. 1(b)). The Launder–Sharma and Nagano–Kim models provided similar predictions (plots are not shown here). The results obtained by using functional c_μ were in better agreement with the experimental data. Computations without the non-linear expansion revealed that the models predictions were mainly dominated by their damping functions and functional c_μ, and it seems that the anisotropic stress expansion does not play any important role in this case. The results using the Spalart–Allmaras model were comparable to those obtained by the non-linear models using functional c_μ. Similar conclusions about the effects of varying c_μ coefficient on turbulence models performance have also been reported in the past for steady compressible flow computations (Bardina et al., 1997; Huang, 1999). All linear k–ϵ models employed in this study predicted the shock position shifted downstream and underestimated the length of separation region. The same was also the case for the algebraic Baldwin–Lomax model (Fig. 1(b)).

In Fig. 2, comparison of numerical and experimental results for the buffet onset is presented. There is a well-defined region of Mach and incidence angle where buffet occurs. Initially, four computations (Fig. 2) were performed at conditions below the experimentally reported buffet onset and steady-state solutions were achieved (symbols in Fig. 2 labelled "no SIO (shock-induced oscillation)"). Afterwards, the incidence-angle was slowly increased to obtain unsteadiness and it was found that after the initial peak of the C_l curve (Fig. 3) the computations resulted either in periodic loads, thus indicating buffet (symbols in Fig. 2 labelled "SIO"), or in steady-state flow. In the latter case, the computations were repeated for a higher incidence-angle until buffet is captured. Once buffet was predicted, the incidence-angle was again decreased and the computation was repeated to check whether the experimental boundary (solid line in Fig. 2) for buffet onset could be closer approached. Computations were performed for a long time interval to verify that almost periodic loads are obtained for the buffet conditions (see Fig. 3(c)).

For all combinations of Mach number and incidence angle considered here, the linear k–ϵ models led to a steady solution (Fig. 3(a), (b)), thus failing to predict buffet. As can be seen in Fig. 2, the computations predict the buffet onset boundary slightly shifted to higher incidence angles and Mach number. This is similar to what Girodroux-Lavigne and LeBalleur (1988) have obtained. Edwards (1996), however, reported results closer to the experimental data using an inverse

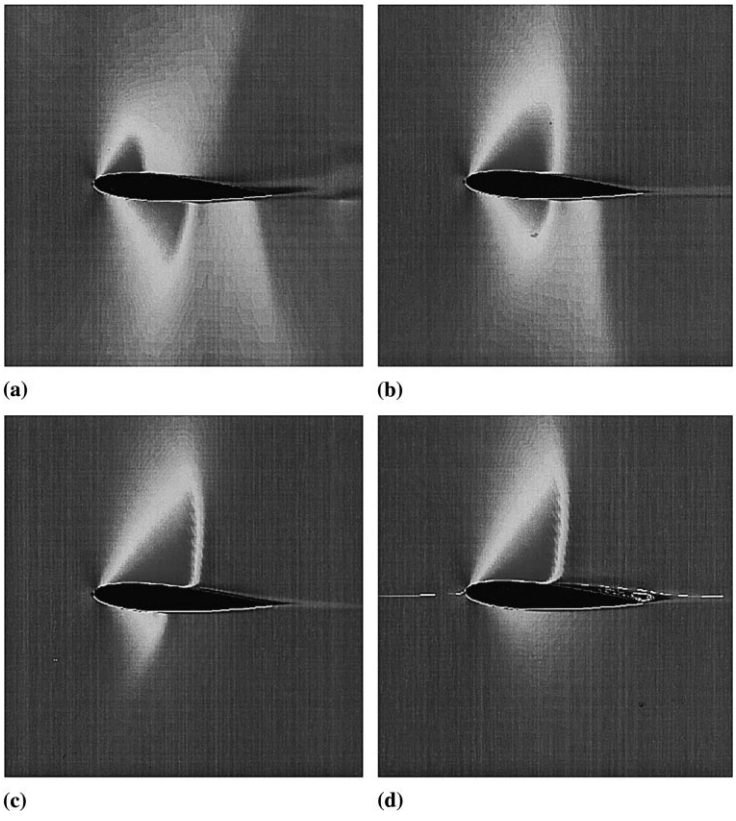

Fig. 4. Mach number field around a NACA-0012 aerofoil at different time instants during the buffet development.

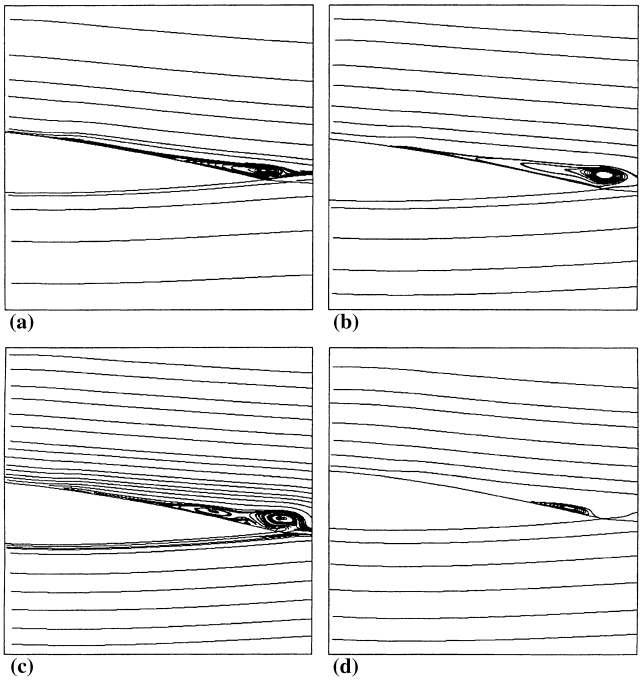

Fig. 5. Separated boundary layer around the trailing edge of a NACA-0012 aerofoil at different time instants during the buffet development.

boundary-layer method and the Baldwin–Lomax (1978) model. He also found that buffet occurs at an angle $\alpha = 0°$ and Mach number close to 0.83.

The Mach number field is shown in Fig. 4 at different time instants during the buffet development and it is clear that the shock formed on the suction side of the profile changes position in time. A much weaker shock is predicted on the pressure side. The separation region close to the trailing edge of the profile is shown in Fig. 5. Initially, the separation region increases and extends both upstream and downstream of the trailing edge of the aerofoil. As the first bubble grows (Fig. 5(b)), a second tiny bubble is formed downstream of the shock (Fig. 5(c)) and starts growing again to repeat the unsteady cycle.

5. Conclusions

Validation and assessment of various turbulence closures were performed in transonic flows around an aerofoil featuring buffet. The results revealed that a functional c_μ coefficient significantly influences the models performance. The non-linear expansion of the shear stress does not seem to improve the predictions. The effects of c_μ was tested in conjunction with the non-linear models because these models have been calibrated for a functional c_μ. It would be worthwhile to use a functional c_μ in conjunction with a linear k–ϵ or k–ω model, but this certainly requires to calibrate first the models coefficients in simpler test cases. Furthermore, the results obtained by the Spalart–Allmaras one equation model were found to be comparable to those obtained by the non-linear models based on functional c_μ.

The buffet computations were found to be computationally more demanding than dynamic-stall computations (Barakos and Drikakis, 1999, 2000a) due to the high resolution in time required to resolve the flow unsteadiness. In addition, to predict the buffet onset several computations need to be performed at different conditions and compare the predicted loads.

Future research needs to address not only modelling issues, but also numerical issues such as the effects of discretization schemes on buffet predictions in transonic flows.

Acknowledgements

The financial support by EPSRC and MOD (GR/L18457) is gratefully acknowledged.

References

Baldwin, B.S., Lomax, H., 1978. Thin layer approximation and algebraic model for separated turbulent flows, AIAA Paper 78-257.

Barakos, G., Drikakis, D., 1998a. Assesment of various low-Re turbulence models in shock boundary layer interaction. Comput. Methods Appl. Mech. Eng. 160 (1–2), 155–174.

Barakos, G., Drikakis, D., 1998b. Implicit-unfactored implementation of two-equation turbulence models in compressible Navier–Stokes methods. Int. J. Numer. Methods Fluids 28 (1), 73–94.

Barakos, G., Drikakis, D., 1999. An implicit unfactored method for unsteady turbulent compressible flows with moving solid boundaries. Comput. Fluids 28 (8), 899–921.

Barakos, G., Drikakis, D., 2000a. Unsteady separated flows over manouvering lifting surfaces, invited paper, Philosophical Transactions of the Royal Society. Ser. A , Mathematical, Physical and Engineering Sciences, to appear.

Barakos, G., Drikakis, D., 2000b. Investigation of non-linear eddy-viscosity models in shock/boundary-layer interaction, AIAA J. 38 (3), 461–469.

Bardina, J.E., Huang, P.G., Coackley, T.J., 1997. Turbulence modeling validation, testing and development, NASA TM 110446, April 1997.

Craft, T.J., Launder, B.E., Suga, K., 1996. Development and application of a cubic eddy-viscosity model of turbulence. Int. J. Heat Fluid Flow 17, 108–115.

Drikakis, D., Durst, F., 1994. Investigation of flux formulae in transonic shock wave/turbulent boundary layer interaction. Int. J. Numer. Methods Fluids 18, 385–413.

Eberle, A., Rizzi, A., Hirschel, E.H., 1992. Numerical Solutions of the Euler Equations for Steady Flow Problems. Springer, Wiesbaden.

Edwards, J.W., 1996. Transonic shock oscillations and wing flutter calculated with an interactive boundary layer coupling method. In: Proceedings of the EUROMECH-Colloquium 349, Simulation of Fluid-Structure Interaction in Aeronautics, Göttingen, Germany.

Girodroux-Lavigne, P., LeBalleur J.C., 1988. Time consistent computation of transonic buffet over airfoils, ONERA TP No. 1988–97.

Haase, W., Brandsma, F., Elsholz, E., Leschziner, M., Schwambron, D. (Eds.), 1993. Euroval, a European initiative on validation of CFD codes. Notes on Numerical Fluid Mechanics, vol. 42. Vieweg, Braunschweig.

Huang, P.G., 1999. Physics and computation of flows with adverse pressure gradients. In: Salas, M.D., Hefner, J.N., Sakell, L. (Eds.), Modeling Complex Turbulent Flows, ICASE/LaRC Interdisciplinary Series in Science and Engineering, vol. 7. Kluwer Academic Publishers, Dordrecht, pp. 245–258.

Launder, B.E., Sharma, B.I., 1974. Application of the energy-dissipation model of turbulence to the calculation of flow near a spinning disk. Lett. Heat Mass Transfer 1, 131–138.

Leschziner, M.A.,1998. Experimental needs for CFD validation. ASME Fluids Engineering Conference, Washington DC, June 1998.

Liou, W.W., Shih, T.H., 1996. Transonic turbulent flow predictions with two-equation turbulence models, NASA CR-198444, ICOMP-96-02, NASA Lewis, OH, USA.

Marvin J.G., Huang, G.P., 1996. Turbulence modeling – progress and future outlook. In: Keynote Lecture Presented at the 15th International Conference on Numerical Methods in Fluid Dynamics, June 1996, Monterey, CA, USA.

Mateer, G.G., Seegmiller, H.L., Hand, L.A., Szodruch, J., 1992. An experimental investigation of a supercritical airfoil at transonic speeds, NASA TM-103933, NASA Ames, CA, USA.

McDevitt, J.B., Okuno, A.F., 1985. Static and dynamic pressure measurements on a NACA 0012 airfoil in the Ames high Reynolds number facility, NASA-TP-2485, NASA Ames, CA, USA.

McDevitt, J.B., Levy Jr., L.L., Deiwert, G.S., 1976. Transonic flow about a thick circular-arc airfoil. AIAA J. 14, 606–613.

Nagano, Y., Kim, C., 1988. A two equation model for heat transport in wall turbulent shear flows. J. Heat Transfer 110, 583–589.

Sofialidis, D., Prinos, P., 1997. Development of a non-linear strain-sensitive k–ω turbulence model. In: Proceedings of the 11th Symposium on Turbulent Shear Flows, TSF-11, Grenoble, France, p2-89–p2-94.

Spalart, P.R, Allmaras, S.R., 1992. A one-equation turbulence model for aerodynamic flows, AIAA Paper 92-0439.